ELSEVIER

Journal of Nuclear Materials 312 (2003) 97–102

journal of nuclear materials

www.elsevier.com/locate/jnucmat

Production behavior of irradiation defects in vitreous silica under ion beam irradiation

Kimikazu Moritani, Ikuji Takagi, Hirotake Moriyama *

Department of Nuclear Engineering, Graduate School of Engineering, Kyoto University, Yoshida-honmachi, Sakyo-ku, Kyoto 606-8501, Japan

Received 24 May 2002; accepted 31 October 2002

Abstract

The production behavior of irradiation defects in vitreous silica was studied by an in situ luminescence measurement technique under ion beam irradiation of H^+ and He^+. No apparent difference was observed in the luminescence spectra of specimens of different OH contents. The temperature dependence of the luminescence intensity at 280 and 460 nm was measured, and analyzed by considering the production mechanisms and kinetics of the irradiation defects of oxygen deficiency centers.

PACS: 61.80.Jh; 78.60.Ya

1. Introduction

Irradiation behavior of ceramic materials is one of the topics of current interest, since some of these materials are to be used in the strong radiation field of proposed fusion reactors. However, the dynamic production behavior of irradiation defects under irradiation has not been fully clarified in spite of the considerable progress in understanding many aspects of irradiation defects in these ceramic materials. It is thus important to know the production behavior of irradiation defects by such an in situ luminescence measurement technique.

For fusion reactor blanket materials, we have already studied the production behavior of irradiation defects in some candidate lithium ceramics by an in situ luminescence measurement technique under ion beam irradiation [1]. In Li_2O, it has been confirmed that the F^+ center (an oxygen vacancy trapping an electron) and the F^0 center (an oxygen vacancy trapping two electrons), which are commonly observed in ionic compounds, are formed by irradiation [2,3]. Similarly, the irradiation defects of oxygen vacancies are produced in Li_2SiO_3 and Li_4SiO_4 [4,5]. These defects are considered to play an important role in the tritium behavior [1].

Following the measurement of lithium ceramics, the present study deals with vitreous silica which is often used as optical fibers in the radiation field. The luminescence spectra were measured under ion beam irradiation, and the temperature dependence of the luminescence intensity was analyzed by considering the production mechanism and kinetics of the irradiation defects.

2. Experimental

Specimens of vitreous silica (T-1030, T-2030, T-4040) of 10 mm in diameter and about 1 mm in thickness were obtained from Toshiba Ceramics Co., and irradiated with H^+ and He^+ ion beam, accelerated to 2 MeV with a Van de Graaff accelerator. The size of the ion beam was about 3 mm in diameter and its current was monitored.

* Corresponding author. Tel./fax: +81-75 753 5824.
E-mail address: moriyama@nucleng.kyoto-u.ac.jp (H. Moriyama).

0022-3115/03/$ - see front matter
PII: S0022-3115(02)01592-1

Table 1
Experimental conditions

Specimen	OH (ppm)	Irradiation condition		
		Projectile	Beam current (nA)	Temperature (K)
T-1030	200	2 MeV He^+	15–50	301–759
T-2030	1	2 MeV He^+	15–50	301–771
T-4040	0.8	2 MeV H^+	20–50	298–919
		2 MeV He^+	15–60	305–851

The luminescence from the target sample was led to monochromaters, Ritsu MC-20N, and counted with photo-multipliers, Hamamatsu R585. The temperature of the sample holder was controlled with an electric heater and a thermocouple while another thermocouple was attached to the sample surface to monitor its temperature. The OH contents of each specimen and the irradiation conditions are summarized in Table 1.

3. Results and discussion

3.1. Luminescence bands

Fig. 1 shows typical luminescence spectra of T-1030, T-2030 and T-4040 under He^+ ion beam irradiation. For comparison, the ordinate represents luminescence intensity normalized to the beam current of 1 nA; the peak heights have been observed to be proportional to the beam current and then all of the spectra in the present study are corrected with the beam current. Similar spectra were also observed for T-4040 under H^+ irradiation. As shown in Fig. 1, the observed luminescence spectra are decomposed into a number of luminescence bands, namely 280, 460 and 490 nm for each vitreous silica. For the decomposition, following the manner in the previous study [5], energy-based Gaussian functions were taken for all the luminescence bands and the peak heights and positions were determined. For a proper convergence, the peak width has been assumed to be given by an empirical correlation that $y = cx^{-2}$ where y denotes the peak width in eV, x the peak position in eV and c a constant.

In the case of SiO_2, there have been reported two types of irradiation defects [6]. One is the oxygen-deficiency-related defects of the so-called E′ centers (≡Si·) and some variants of oxygen deficiency centers (ODCs, ≡Si:Si≡), and the other the oxygen-excess-related defects such as the non-bridging oxygen hole centers (≡Si–O·) and the peroxy radicals (≡Si–O–O·). As for the luminescence of irradiation defects, it is known that the luminescence of ODCs is observed at the UV region around 2.7 eV (460 nm) and 4.4 eV (280 nm) while that of the others like the non-bridging oxygen hole centers is observed at rather low photon energy region. Thus the

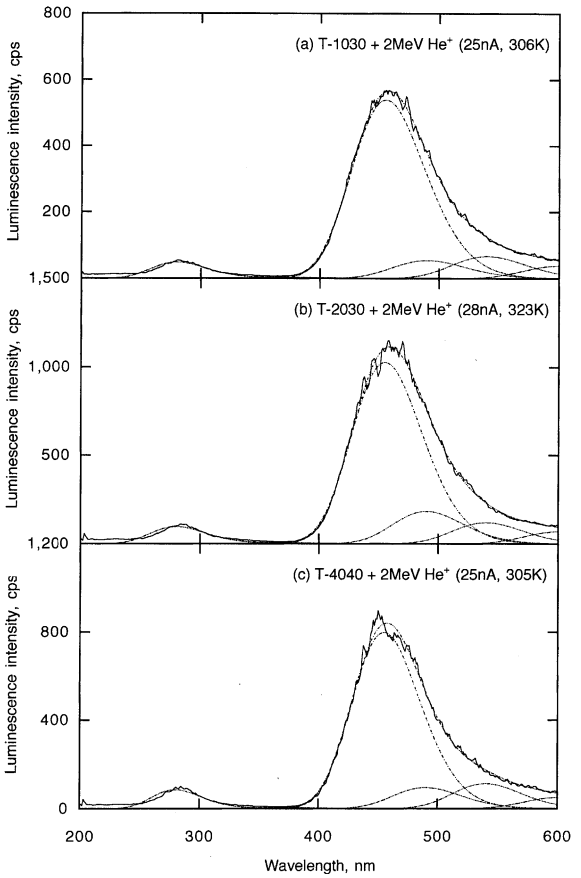

Fig. 1. Typical luminescence spectra of T-1030, T-2030 and T-4040 under 2 MeV He^+ ion beam irradiation. The ordinate represents luminescence intensity normalized to the beam current of 1 nA. The dashed curves represent the results of decomposition as described in Section 3.1.

presently observed luminescence from SiO_2 which is centered at 280 and 460 nm can be attributed to ODCs. As already suggested in our previous study [5], the luminescence intensity is linearly dependent not only on electronic excitation rate [7] but also on displacement rate [8], and it is reasonable to assume that the luminescence comes from the relaxation process of newly formed ODCs trapping electrons.

As shown in Fig. 1, no apparent difference was observed in the luminescence spectra of the specimens of different OH contents. This means that the OH does not play so important role in the present luminescence behavior.

3.2. Temperature dependence of luminescence intensity

Figs. 2–4 show the Arrhenius plots of the luminescence intensity at fixed bands for T-1030, T-2030 and T-4040, respectively. As shown in these figures, the intensity decreases rather monotonically with temperature. This is a little different result from that of the previous study [5], in which some non-monotonic temperature dependence has been observed for the luminescence at 460 nm from T-1030. According to the previous study [5], however, such a non-monotonic temperature dependence is due to the contribution of irradiation defects which are easily saturated, and then this difference is explained by considering different beam currents between two cases. In fact, the beam current of 20–50 nA in the present study is much higher than that of 3 nA in the previous study. The irradiation defects might be so saturated that their contribution could not been observed in the present study. The present result of the temperature dependence is thus consistent with the previous one.

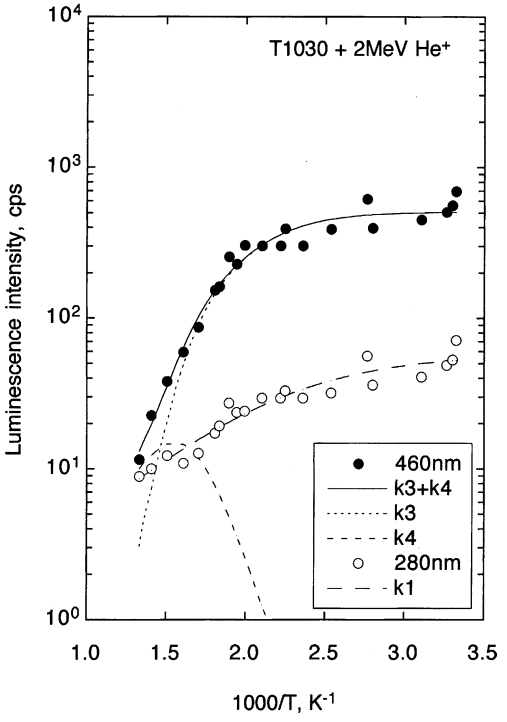

Fig. 2. Arrhenius plots of luminscence intensity of T-1030 under 2 MeV He^+ irradiation. The ordinate represents luminescence intensity normalized to the beam current of 1nA. The marks are experimental and the curves represent the least-squares fits of the data to Eqs. (7) and (8) as described in Section 3.4.

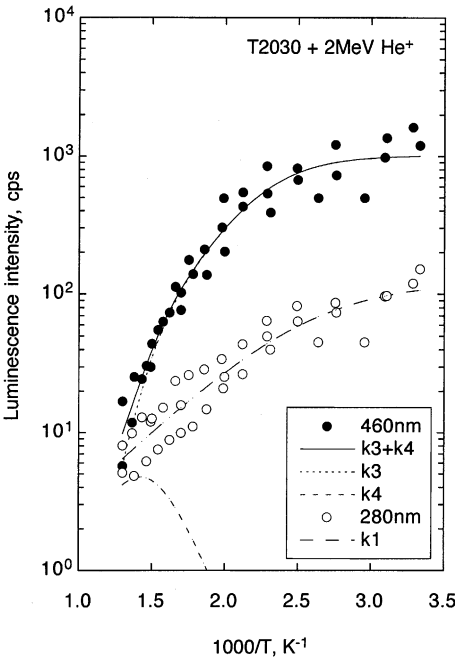

Fig. 3. Arrhenius plots of luminscence intensity of T-2030 under 2 MeV He^+ irradiation. See also Fig. 2 caption.

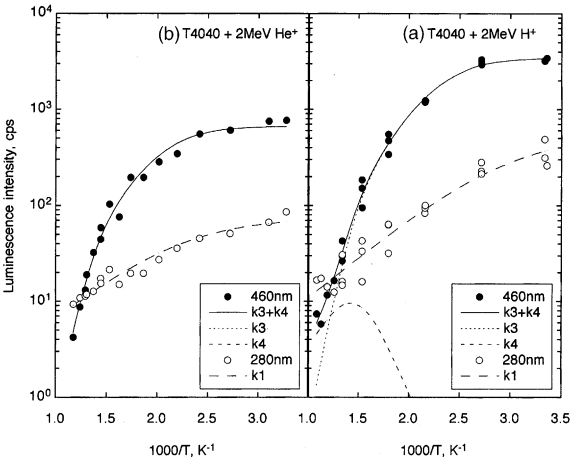

Fig. 4. Arrhenius plots of luminscence intensity of T-4040 under (a) H^+ and (b) He^+ irradiation. See also Fig. 2 caption.

For confirmation, the result of the previous study [5] was re-examined here in some details. In that study, the luminescence intensity was measured by increasing temperature up to 830 K and then by decreasing temperature to ambient one, and an interesting temperature

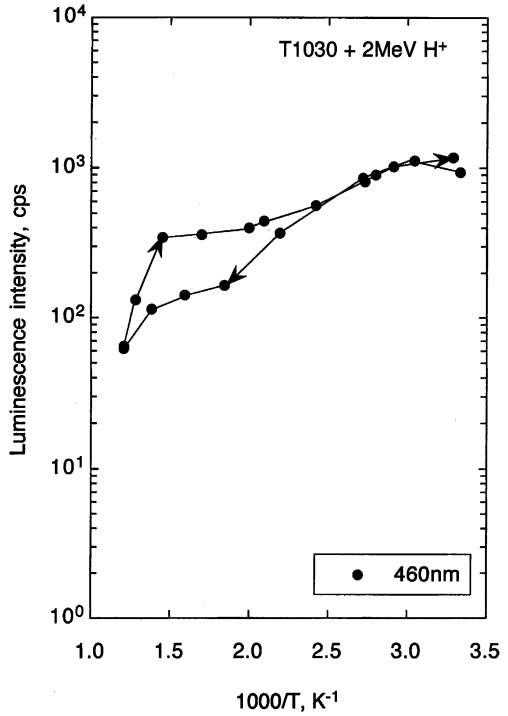

Fig. 5. Arrhenius plots of luminscence intensity of T-1030 under 2 MeV He^+ irradiation with a low beam current of 3 nA [5].

dependence of the luminescence intensity was found in the temperature region above 450 K as shown in Fig. 5. It can be seen that the luminescence intensity with decreasing temperature is a little higher than that with increasing temperature in this region. This hysteresis effect can be explained by considering the irradiation history. According to the previous study [5], a considerable part of the luminescence in this region is attributed to the formation of ODCs accompanied with peroxy linkages, which are likely to be saturated by irradiation. Thus it can be considered that the luminescence intensity with increasing temperature is reduced by the effect of saturation while the luminescence with decreasing temperature is increased by the recovery of peroxy linkages at the higher temperature.

3.3. Production mechanism of irradiation defects

As is known [6], the luminescence at 2.7 eV (460 nm) and 4.4 eV (280 nm) is attributed to the triplet (T_1 to S_0) and the singlet (S_1 to S_0) emissions of ODCs. It is also known that the singlet–triplet conversion (S_1 to T_2) occurs with the activation energy of 0.13 eV [6], and that the luminescence at 460 nm is due to the formation of ODCs accompanied with the formation of peroxy linkages (–O–) and/or oxygen interstitials (O_i) [5]. By considering these known facts, the following production mechanism of irradiation defects in SiO_2 can be suggested:

$$SiO_2 \rightarrow SiO_2^* \rightarrow ODC(S_1), ODC(T_1) \quad (0)$$

$$ODC(S_1) \rightarrow ODC(S_0) + h\nu_{280} \quad (1)$$

$$ODC(S_1) \rightarrow ODC(T_2) \rightarrow ODC(T_1) \quad (2)$$

$$ODC(T_1) \rightarrow ODC(S_0) + O_i + h\nu_{460} \quad (3)$$

$$ODC(T_1) \rightarrow ODC(S_0) + (\text{–O–}) + h\nu_{460} \quad (4)$$

$$ODC(T_1) \rightarrow \text{recombination with } O_i \quad (5)$$

$$ODC(T_1) \rightarrow \text{recombination with (–O–)} \quad (6)$$

As shown in Fig. 6, reaction (0) represents the production of an excited SiO_2 (SiO_2^*) by ion beam irradiation, which is de-excited to $ODC(S_1)$ and $ODC(T_1)$. Reaction (1) represents the de-excitation of the $ODC(S_1)$ accompanied with the luminescence at 280 nm, and reaction (2) the singlet–triplet conversion [6]. Because of rather monotonic temperature dependence of the 280 nm luminescence, no other reaction is considered for the $ODC(S_1)$. According to the previous study [5], on the other hand, a number of competitive reactions are considered for the 460 nm luminescence, namely reactions (3)–(6). Reactions (3) and (4) represent the de-excitation of the $ODC(T_1)$ accompanied with the

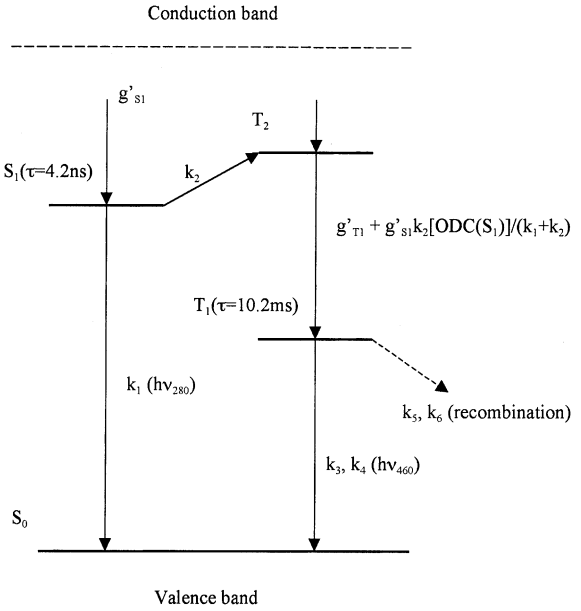

Fig. 6. Flat-band diagram of vitreous silica summarizing the relative energy positions of ODCs.

formation of an oxygen interstitial (O_i) and a peroxy linkage (–O–), respectively, and reactions (5) and (6) the recombination with the oxygen interstitial and peroxy linkage, respectively.

Reaction (4) requires some thermal activation and will take place at high temperatures since the moved oxygen atom is incorporated into a peroxy linkage. This is the reason why the luminescence at 460 nm has been observed at high temperatures in our previous study [5]. In the present case, however, the contribution of these reactions is considered to be much smaller as mentioned above.

3.4. Determination of kinetic parameters

It is interesting and important to obtain the rate constants of reactions involved in the production of irradiation defects. Based on the suggested reaction scheme, the observed temperature dependence of the luminescence intensity is analyzed here.

Following the reaction scheme, the observed luminescence intensities I_{280} and I_{460} at 280 nm and 460 nm are expressed as:

$$I_{280} = k_1[\mathrm{ODC}(S_1)], \tag{7}$$

$$I_{460} = k_3[\mathrm{ODC}(T_1)] + k_4[\mathrm{ODC}(T_1)], \tag{8}$$

where k_i is the rate constant of reaction (i). The lifetimes of $\mathrm{ODC}(S_1)$ and $\mathrm{ODC}(T_1)$ are assumed to be very short and a steady-state approximation is applied to these ODCs, that is:

$$\mathrm{d}[\mathrm{ODC}(S_1)]/\mathrm{d}t = g'_{S_1} - k_1[\mathrm{ODC}(S_1)] - k_2[\mathrm{ODC}(S_1)] = 0, \tag{9}$$

$$\mathrm{d}[\mathrm{ODC}(T_1)]/\mathrm{d}t = g'_{T_1} + k_2[\mathrm{ODC}(S_1)] - k_3[\mathrm{ODC}(T_1)] - k_4[\mathrm{ODC}(T_1)] - k_5[\mathrm{ODC}(T_1)] - k_6[\mathrm{ODC}(T_1)] = 0, \tag{10}$$

where g'_{S_1} and g'_{T_1} are the apparent generation rate of $\mathrm{ODC}(S_1)$ and $\mathrm{ODC}(T_1)$ by reaction (0). For simplicity, reactions (5) and (6) are assumed to be the first-order reactions in the present study. In order to calculate the luminescence intensities, the steady-state concentrations of $\mathrm{ODC}(S_1)$ and $\mathrm{ODC}(T_1)$ are obtained from Eqs. (9) and (10), respectively, and substituted into Eqs. (7) and (8), respectively.

In the present analysis, the obtained data for the temperature dependence of the luminescence intensity are fitted to Eqs. (7) and (8) by least-squares method. The rate constants are assumed to be of the Arrhenius type and hence the pre-exponential term A_i and activation energy term E_i are determined. For a proper convergence, however, the number of free parameters is reduced as much as possible. Fortunately, the activation energies for reactions (4)–(6) have been determined in the previous study [6], and are assumed to be the same for all specimens in the present study by considering the similarities in the temperature dependence of the luminescence as shown in Figs. 2–4. Then, the pre-exponential terms and the generation rates are treated as fitting parameters in the present study. As shown in

Table 2
Optimum parameter values obtained from the analysis of in situ luminescence measurement data

Specimen	Projectile	$k_2/k_1 = A_2/A_1 \exp[-(E_2-E_1)/RT]$		g'_{S_1} (s^{-1})				g'_{T_1} (s^{-1})
		A_2/A_1 (–)	E_2-E_1 (kJ/mol)					
T-1030	He^+	8.4×10^1	16.8	5.8×10^1				
T-2030	He^+	3.8×10^2	19.5	1.2×10^2				
T-4040	H^+	3.6×10^2	16.5	5.5×10^2				
	He^+	7.5×10^1	16.5[a]	7.5×10^1				
		$k_4/k_3 = A_4/A_3 \exp[-(E_4-E_3)/RT]$		$k_5/k_3 = A_5/A_3 \exp[-(E_5-E_3)/RT]$		$k_6/k_3 = A_6/A_3 \exp[-(E_4-E_3)/RT]$		
		A_4/A_3 (–)	E_4-E_1 (kJ/mol)	A_5/A_3 (–)	E_5-E_3 (kJ/mol)	A_6/A_3 (–)	E_6-E_3 (kJ/mol)	
T-1030 [5]	H^+	9.8×10^6	72.0	3.4×10^3	32.4	1.1×10^{10}	104.1	9.6×10^2
T-1030	He^+	3.2×10^5	72.0[b]	2.3×10^3	32.4[b]	2.4×10^9	104.1[b]	5.1×10^2
T-2030	He^+	5.5×10^4	72.0[b]	5.7×10^3	32.4[b]	1.6×10^9	104.1[b]	1.0×10^3
T-4040	H^+	4.1×10^4	72.0[b]	7.1×10^3	32.4[b]	2.0×10^9	104.1[b]	3.4×10^3
	He^+	–[c]	72.0[b]	2.6×10^3	32.4[b]	2.7×10^8	104.1[b]	6.6×10^2

[a] Assumed to be the same for both H^+ and He^+ ion irradiations of each specimen.
[b] Taken from the previous study [5] and assumed to be the same for all specimens.
[c] Negligible.

Figs. 2–4, the observed temperature dependence of the luminescence intensity is well fitted to Eqs. (7) and (8), and the values of kinetic parameters of the involved reactions are obtained as given in Table 2.

The activation energy value of reaction (2) is obtained to be 16.8 kJ/mol (0.17 eV), 19.5 kJ/mol (0.20 eV), 16.5 kJ/mol (0.17 eV) for T-1030, T-2030, T-4040, respectively. These values are found to be consistent with the reported value of 0.13 eV for the singlet–triplet conversion [9], supporting the present interpretation of observations. Although no other reaction is considered for the 280 nm luminescence in the present study, this is also consistent with a very short lifetime ($\tau = 4.2$ ns [10,11]) of the ODC(S_1). In such a case, its recombination reaction is considered to hardly occur since it needs a longer time for the diffusion of oxygen interstitials and peroxy linkages. In the case of the 460 nm luminescence, on the other hand, the lifetime of the ODC(T_1) is much longer ($\tau = 10.2$ ms [12,13]) and then its recombination reactions will occur as observed in the present study.

4. Conclusions

In order to know the production behavior of irradiation defects in vitreous silica, the temperature dependence of the luminescence intensity was studied by an in situ luminescence technique. The temperature dependence of the 280 nm luminescence was well explained by considering the radiative transition of ODC(S_1) to ODC(S_0) competing only with the singlet–triplet conversion of ODC(S_1). In the case of the 460 nm luminescence, on the other hand, its temperature dependence was interpreted by considering a number of competing reactions including its recombination with oxygen interstitials and peroxy linkages. The different temperature dependence is due to different lifetimes of the two states, and the lifetime of the ODC(S_1) seems to be too short to recombine with oxygen interstitials and peroxy linkages.

Acknowledgement

The authors wish to thank Mr K. Yoshida, Kyoto University, for his kind experimental supports.

References

[1] H. Moriyama, S. Tanaka, K. Noda, J. Nucl. Mater. 258–263 (1998) 587.
[2] Y. Asaoka, H. Moriyama, K. Iwasaki, K. Moritani, Y. Ito, J. Nucl. Mater. 183 (1991) 174.
[3] Y. Asaoka, H. Moriyama, Y. Ito, Fusion Technol. 21 (1992) 1944.
[4] H. Moriyama, T. Nagae, K. Moritani, Y. Ito, Nucl. Instrum. and Meth. B 91 (1994) 317.
[5] K. Moritani, S. Tanaka, H. Moriyama, J. Nucl. Mater. 281 (2000) 106.
[6] L. Skuja, J. Non-Cryst. Solids 239 (1998) 16.
[7] M. Fujiwara, T. Tanabe, H. Miyamaru, K. Miyazaki, Nucl. Instrum. and Meth. B 116 (1996) 536.
[8] T. Tanabe, A. Omori, M. Fujiwara, J. Nucl. Mater. 258–263 (1998) 1914.
[9] L. Skuja, J. Non-Cryst. Solids 167 (1994) 229.
[10] H. Nishikawa, E. Watanabe, D. Ito, Y. Ohki, Phys. Rev. Lett. 72 (1994) 2101.
[11] R. Boscanio, M. Cannas, F.M. Gelardi, M. Leone, J. Phys.: Condens. Matt. 8 (1996) L545.
[12] L.N. Skuja, A.N. Streletsky, A.B. Pakovich, Solid State Commun. 50 (1984) 1069.
[13] L. Skuja, J. Non-Cryst. Solids 149 (1992) 77.